Characteristics of diffusion-weighted images and apparent diffusion coefficients of ranulas and other masses in and around the floor of the mouth

Nao Wakasugi-Sato, DDS, PhD,[a] Manabu Habu, DDS, PhD,[b] Masafumi Oda, DDS, PhD,[a] Tatsurou Tanaka, DDS, PhD,[a] Ikuko Nishida, DDS, PhD,[c] Tetsuro Wakasugi, MD, PhD,[d] Shinya Kokuryo, DDS, PhD,[e] Daigo Yoshiga, DDS, PhD,[e] Teppei Sago, DDS, PhD,[f] Nozomu Harano, DDS, PhD,[f] Shinji Kito, DDS, PhD,[a] Shinobu Matsumoto-Takeda, DDS, PhD,[a] Takaaki Jyoujima, DDS,[a] Yuichi Miyamura, DDS,[a] Naomi Yada, DDS, PhD,[g] Masaaki Sasaguri, DDS, PhD,[b] and Yasuhiro Morimoto, DDS, PhD[a]

Objective. The aim of this study was to evaluate the characteristics of diffusion-weighted imaging (DWI) and apparent diffusion coefficient (ADC) values of ranulas. In addition, to elucidate DWI findings and ADC values of other representative masses in and around the floor of the mouth.

Study Design. DWI findings and ADC values in 35 patients with ranulas and 33 patients with other masses were retrospectively reviewed with a central focus on cystic masses or lesions that may have cyst-like components in and around the floor of the mouth based on the diagnosis of each respective disease.

Results. Ranulas were all well-defined, homogeneous masses with high signal intensity on DWI. The mean ± standard deviation ADC value of the 35 ranulas was $2.59 \pm 0.31 \times 10^{-3}$ mm^2/s. There was a significant difference in ADC values between simple and plunging ranulas. On DWI, most other masses were heterogeneous, and most ADC values, except those for thyroglossal duct cysts, hemangiomas, and pleomorphic adenomas, were significantly lower than those for ranulas.

Conclusions. The characteristic DWI and ADC findings of ranulas can be determined accurately, and these data can be significantly useful in the differential diagnosis of many kinds of diseases in and around the oral floor. (Oral Surg Oral Med Oral Pathol Oral Radiol 2019;127:77−84)

The utility of diffusion-weighted imaging (DWI) and apparent diffusion coefficients (ADCs) in magnetic resonance imaging (MRI) for the examination of acute cerebral ischemia is widely accepted in the medical field. DWI and ADCs are also thought to be of clinical value in the oral and maxillofacial region in the diagnosis of conditions resulting from infectious diseases, neoplasms, trauma, and metabolic diseases.[1-5]

This study was supported in part by grants-in-aid for scientific research from the Ministry of Education, Science, Sports and Culture of Japan to YM.

[a]Division of Oral and Maxillofacial Radiology, Kyushu Dental University, Kitakyushu, Japan.
[b]Division of Maxillofacial Surgery, Kyushu Dental University, Kitakyushu, Japan.
[c]Division of Developmental Stomatognathic Function Science, Kyushu Dental University, Kitakyushu, Japan.
[d]Division of Otorhinolaryngology-Head and Neck Surgery, University of Environmental Health, Kitakyushu, Japan.
[e]Division of Oral Medicine, Kyushu Dental University, Kitakyushu, Japan.
[f]Division of Dental Anesthesiology, Kyushu Dental University, Kitakyushu, Japan.
[g]Division of Oral Pathology, Kyushu Dental University, Kitakyushu, Japan.

Received for publication Mar 16, 2018; returned for revision Aug 29, 2018; accepted for publication Sep 1, 2018.

2212-4403/$-see front matter
http://doi.org/10.1016/j.oooo.2018.09.002

The area in and around the floor of the oral cavity is located close to the sublingual glands, nerves, tongue, and muscles that play important roles in digestion and speech. Many kinds of diseases, such as ranulas, epidermoid and thyroglossal duct cysts, hemangiomas, sublingual gland−related tumors, carcinoma, and inflammatory lesions, originate in and around the oral floor. Differential diagnoses of these diseases can be very difficult because of the many kinds of tissues involved and the complex anatomy. In particular, if the lesions are relatively small, differentiating among the various lesions in and around oral cavity floor can be very difficult. MRI is very useful in the differential diagnoses of these lesions, including ranulas, because it has much higher contrast resolution between soft tissues and is a noninvasive modality without X-ray exposure.[6] Thus, DWI and ADCs have been clinically applied in the process of formulating differential diagnoses. There have been some reports of DWI findings

Statement of Clinical Relevance

The characteristic findings on diffusion-weighted imaging and the apparent diffusion coefficient values of ranulas can be determined accurately, and these data can be significantly useful in the differential diagnosis of many kinds of diseases of the oral floor.

and ADC values of malignant and benign tumors.[7-9] However, to the best of our knowledge, there have been no reports of the characteristic DWI findings and ADC values of ranulas and other masses in and around the floor of the mouth.

The purpose of the present study was to evaluate the characteristics of DWI and ADC values of ranulas. In addition, the characteristic DWI findings and ADC values of other lesions were compared with those of ranulas to facilitate the differential diagnoses of masses in and around the floor of the oral cavity, with a focus on lesions with cyst-like components.

MATERIALS AND METHODS

We conducted a retrospective investigation of patients who visited Kyushu Dental University Hospital from July 2011 to June 2016 and underwent MRI for lesions in and around the floor of the mouth. The sample population included 35 patients with ranulas (26 simple ranulas, 9 plunging ranulas; 18 males, 17 females; mean age 32.1 years; age range 7−78 years) and 33 patients with masses other than ranulas (15 males, 18 females; mean age 53.5 years; age range 11−92 years). The lesions in the second group were cysts or cyst-like abnormalities located in (n = 17) and around (n = 16) the oral floor. These lesions included epidermoid cysts, thyroglossal duct cysts, hemangiomas, pleomorphic adenomas, squamous cell carcinomas, adenoid cystic carcinomas, and inflammatory diseases. The data from the patients with ranulas and from those with other masses are shown in Table I. A total of 23 ranulas and 11 mass lesions were evaluated microscopically on pathologic examination after surgical procedures. The clinical diagnoses of the cases that could not be diagnosed microscopically were reported if surgical procedures were not performed. Eight simple ranulas, 4 plunging ranulas, 8 hemangiomas, 4 epidermoid cysts, 4 thyroglossal duct cysts, and 7 cases of inflammation were diagnosed clinically.

T1-weighted (T1WI), short-T1 inversion recovery (STIR), DWI, and ADC maps were obtained at the MRI examinations. The imaging parameters used in these sequences are shown in Table II. Contrast MRI scans with gadolinium are acquired in our hospital only when malignant tumors are suspected. These scans are not obtained for benign lesions because of the risk of side effects caused by the contrast medium. The 4 types of MRI images (T1WI, STIR, DWI, and ADC maps) mentioned above were obtained for all of the patients in the present study, whether the masses were benign or malignant. For the MRI examinations, verbal informed consent was obtained from all adult patients and from the parents or guardians of minors. The Human Investigations Committee of Kyushu Dental University ensured that individuals' rights were protected. Approval of the present study was obtained from the institutional review board of Kyushu Dental University (No. 13-19).

All images were acquired by using a 1.5-T full-body MR system (EXCELART Vantage Powered by Atlas; Toshiba, Tokyo, Japan) with a circular polarized neck coil to visualize specific areas of the floor of the mouth. DWI was performed by using single-shot multiecho parallel echo planar imaging. Other scanning parameters are shown in Table II. Conventional single-section sagittal,

Table II. Imaging parameters

	Sequences		
	T1WI	*STIR*	*DWI*
TR (ms)	820	4700	5500
TE (ms)	15	75	95
Flip angle/flop angle (°)	90/160	90/160	90/180
FOV (mm)	200 × 256	200 × 200	200 × 200
Section thickness (mm)	6.0	6.0	6.0
Intersection gap (mm)	1.2	1.2	1.2
Slab thickness (mm)	7.2 × 15	7.2 × 15	7.2 × 15
Matrix (pixels)	224 × 320	272 × 272	144 × 144
B factor			1000

DWI, diffusion-weighted images; *FOV,* field of view; *STIR,* short-TI inversion recovery; *T1WI,* T1-weighted images; *TE,* time of echo; *TR,* time of repetition.

Table I. Pathologic and clinical diagnosis, age, and sex of 68 patients with cystic mass or lesions having cyst-like components in and around the floor of the mouth

Category	*Diagnosis*	*Age (y)*	*Male/Female*
Pseudocysts (n = 35)	Ranulas	32.1 ± 19.3	18/17
	Simple ranulas (n = 26)	33.8 ± 21.8	11/15
	Plunging ranulas (n = 9)	27.2 ± 8.1	7/2
Cysts (n = 7)	Epidermoid cysts (n = 4)	33.0 ± 19.4	1/3
	Thyroglossal duct cysts (n=3)	29.6 ± 17.6	0/3
Benign tumors (n = 11)	Hemangiomas (n=8)	47.9 ± 19.9	4/4
	Pleomorphic adenomas (n = 3)	70.0 ± 5.3	0/3
Malignant tumors (n = 8)	Carcinomas (n = 6)	63.0 ± 11.0	5/1
	Adenoid cystic carcinomas (n = 2)	78.5 ± 9.2	2/0
Inflammation (n = 7)	Inflammation (n = 7)	61.4 ± 21.7	2/5

coronal, and transverse MRI scans of the oral and maxillofacial regions were obtained initially. The acquisition slab was oriented in the transverse direction on the sagittal and coronal images so that ranulas and other diseases in and around the oral floor could be included.

In patients with ranulas and other diseases of the floor of the mouth, characteristic DWI findings and ADC values were evaluated. ADCs were calculated, pixel by pixel, for areas with high signals indicative of ranulas on axial STIR images. In addition, ADC maps were prepared. Moreover, the extent, margins, internal architecture, and signal intensity were also investigated on T1-weighted and STIR images according to Kurabayashi et al.[6] The MRI scans were independently assessed by 2 research radiologists (N.W. and M.O.). Both are expert radiologists: N.W. with 12 years of experience and M.O. with 11 years of experience are both specialists certified by the Japanese Society for Oral and Maxillofacial Radiology. The extent, margins, internal architectures, and signal intensity on the MRI scans were judged by these 2 expert radiologists. In case of disagreement, a final assessment was reached by consensus after discussion. All statistical tests, such as the Student *t* test for the analysis between 2 groups, Pearson's correlation coefficient, and analysis of variance (ANOVA) to compare more than 2 groups, such as ADC values and MRI findings between ranulas and other lesions, were performed by using the SPSS software, version 11 (SPSS Inc., Chicago, IL). The level of significance was $P < .05$. Correlations from Pearson's analysis were classified into 5 grades: very weak, 0.00 to ±0.20; weak, ±0.21 to ±0.40; moderate, ±0.41 to ±0.70; strong, ±0.71 to ±0.90; and very strong, ±0.91 to ±1.00.

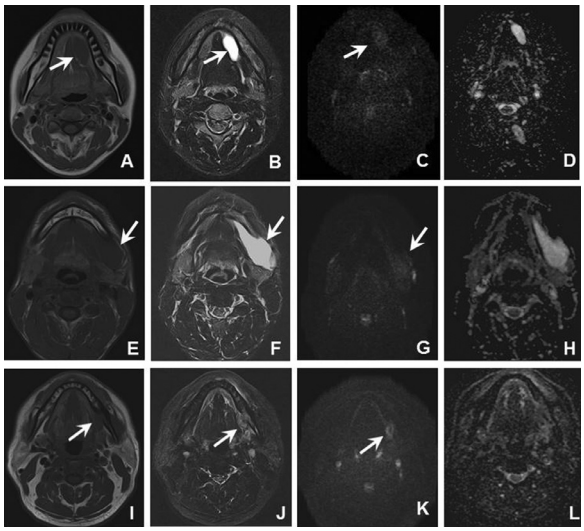

Fig. 1. Simple ranulas **(A, B, C, D)**, plunging ranulas **(E, F, G, H)**, and squamous cell carcinomas **(I, J, K, L)** on MRI. T1WI **(A)**, STIR **(B)**, and DWI **(C)** show well-defined masses confined to the sublingual space *(arrow)*. A homogeneous low signal is seen on T1WI, with high signals on STIR and DWI (A, B, C). The ADC map of simple ranulas (D) shows a value of 2.46×10^{-3} mm^2/s. T1WI (E), STIR (F), and DWI (G) show well-defined masses in the sublingual and submandibular spaces (*arrow*). A homogeneous low signal is seen on T1WI, with high signals on STIR and DWI (E, F, G). The ADC map of a plunging ranula (H) shows an ADC value of 2.73×10^{-3} mm^2/s. T1WI (I), STIR (J), and DWI (K) show unclear and irregular masses in the sublingual and submandibular spaces (*arrow*). Squamous cell carcinomas had heterogeneous high signal intensity on STIR and DWI (I, J). The ADC map of a squamous cell carcinoma (L) shows an ADC value of 0.93×10^{-3} mm^2/s. *ADC,* apparent diffusion coefficient; *DWI,* diffusion-weighted imaging; *MRI,* magnetic resonance imaging; *STIR,* short-T1 inversion recovery; *TIWI,* T1 weighted imaging.

RESULTS

Characteristic findings on MRI, including DWI of ranulas and other lesions

On MRI, the 35 ranulas were well-defined homogeneous masses with low signal intensity on T1WI and high signal intensity on STIR (Figure 1). On DWI, the 35 ranulas were relatively homogeneous, with high signal intensity (see Figure 1). The 26 simple ranulas were all confined to the sublingual space and relatively small. The 9 plunging ranulas were centered on the submandibular space and were likely to spill into one or more adjacent spaces, such as the sublingual and parapharyngeal spaces. MRI findings, including DWI, such as extent, margins, internal architecture, and signal intensity, of simple ranulas were similar to those of plunging ranulas (see Figure 1; Table III). Plunging ranulas extended slightly into the sublingual space, the so-called tail sign, in 6 of 9 cases. There were no differences in the MRI findings of ranulas between males and females or between age groups, as illustrated in Figure 2.

The MRI findings of all other masses in the present study were different from those of ranulas in one or more ways. MRI findings of epidermoid cysts were mostly similar to those of ranulas. However, they were oval or round, unlike ranulas (Figure 3). For epidermoid cysts, no superior extension into the parapharyngeal space was found in any case. In addition, the signal intensity of one case on T1WI was medium intensity (see Table III). Thyroglossal duct cysts were located in the midline of the oral floor, and they did not extend to the sublingual glands. DWI findings of thyroglossal duct cysts were not similar to those of ranulas, as 2 of the 3 lesions had heterogeneous high signal intensity (see Figure 3 and Table III).

Table III. Statistical data for 68 cystic mass or lesions having cyst-like components in and around the floor of the mouth

Category	*Diagnosis*	*Mean ± SD value of ADC*	*Extent*		*Margin*		*IA*			*Hom*		*T1WI*			*STIR*		
		(× 10^{-3} mm^2/s)	*O*	*MS*	*R*	*I*	*U*	*Ml*	*Ho*	*He*	*L*	*M*	*H*	*L*	*H*
Pseudocysts	Ranulas (n = 35)	2.59 ± 0.31	30	5	35	0	35	0	35	0	35	0	0	0	35
	Simple ranulas (n = 26)	2.52 ± 0.30*	26	0	26	0	26	0	26	0	26	0	0	0	26
	Plunging ranulas (n = 9)	2.79 ± 0.27	4	5	9	0	9	0	9	0	9	0	0	0	9
Cysts	Epidermoid cysts (n = 4)	1.55 ± 1.40†	3	1	4	0	4	0	4	0	3	1	0	0	4
	Thyroglossal duct cysts (n = 3)	2.16 ± 0.30	3	0	3	0	1	2	1	2	1	2	0	0	3
Benign tumors	Hemangioma (n = 8)	2.24 ± 0.66	4	4	6	2	3	5	6	2	5	3	0	0	8
	Pleomorphic adenomas (n = 3)	1.84 ± 0.50	3	0	2	1	0	3	3	0	3	0	0	0	3
Malignant tumors	Carcinomas (n = 6)	1.02 ± 0.18‡	1	5	2	4	2	4	2	4	6	0	0	0	6
	Adenoid cystic carcinomas (n = 2)	1.44 ± 0.20‡	2	0	1	1	2	0	2	0	2	0	0	0	2
Inflammations	(n = 7)	1.53 ± 0.76‡	1	6	0	7	–	–	1	6	3	4	0	0	7

*Significant difference between simple and plunging ranulas determined by using the Student *t* test; *P* = .004.
†Significant differences vs ranula determined by using analysis of variance (ANOVA); *P* = .010.
‡Significant differences vs ranula determined by using (ANOVA); *P* < .001.
H, high; *He,* heterogeneous; *Ho,* homogeneous; *Hom,* homogeneity; *I,* irregular; *IA,* internal architecture; *L,* low; *M,* medium; *MI,* multilocular; *MS,* multiple spaces; *O,* one space; *R,* regular; *SD,* standard deviation; *STIR,* signal intensity on STIR; *T1WI,* signal intensity on T1WI; *U,* unilocular.

Fig. 2. Differences of simple ranulas by sex and age on DWI (A, B, C, D) and in ADC values (E, F, G, H). DWI in a 13-year-old girl with a simple ranula (A), DWI in a 14-year-old boy with a simple ranula (B), DWI in a 54-year-old woman with a simple ranula (C), and DWI in a 52-year-old man with a simple ranula (D), all show well-defined masses confined to the sublingual space (*arrow*). The ADC map of a 13-year-old girl with a simple ranula (E, 2.82×10^{-3} mm^2/s), the ADC map of an 11-year-old boy with a simple ranula (F, 2.36×10^{-3} mm^2/s), the ADC map of a 54-year-old woman with a simple ranula (G, 2.94×10^{-3} mm^2/s), and the ADC map of a 52-year-old man with a simple ranula (H, 2.45×10^{-3} mm^2/s). *ADC,* apparent diffusion coefficient; *DWI,* diffusion-weighted imaging.

Fig. 3. The MRI findings of an epidermoid cyst (A, B, C) and a thyroglossal duct cyst (D, E, F) as examples of cystic masses or lesions that may have cyst-like components other than ranulas on STIR (A, D), DWI (B, E), and the ADC map (C, F). The epidermoid cyst had an oval outline, unlike ranulas (A, B). The ADC map of the epidermoid cyst (C) showed a value of 1.39×10^{-3} mm^2/s, lower than that of ranulas. The ADC values of these cysts were significantly lower than those for ranulas. Thyroglossal duct cysts were located in the midline of the oral floor, and they did not continue to the sublingual glands (D, E). The ADC map of the thyroglossal duct cyst (F), had an ADC value of 2.48×10^{-3} mm^2/s, relatively similar to ranulas. The ADC values of thyroglossal duct cysts were not significantly different from ranulas. *ADC,* apparent diffusion coefficient; *DWI,* diffusion-weighted imaging; *MRI,* magnetic resonance imaging; *STIR,* short-T1 inversion recovery.

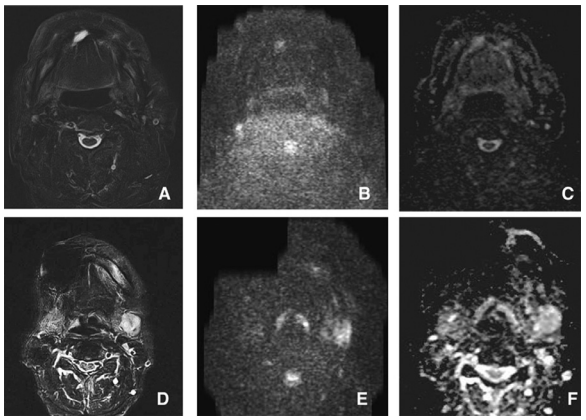

Fig. 4. The MRI findings of a hemangioma (A, B, C) and a pleomorphic adenoma (D, E, F) as benign tumors representing lesions that may have cyst-like components other than ranulas on STIR (A, D), DWI (B, E), and the ADC map (C, F). The hemangiomas showed heterogeneous high signal intensity (A, B). The ADC map of the hemangioma (C) with an ADC value of 2.24×10^{-3} mm^2/s was relatively similar to ranulas. No significant differences were found in ADC values between hemangiomas and ranulas. Pleomorphic adenomas had heterogeneous high signal intensity on STIR and DWI (D, E). The ADC map of the pleomorphic adenoma (F) had a value of 1.35×10^{-3} mm^2/s, lower than that of ranulas, although no significant differences were found in ADC values between these lesions. *ADC,* apparent diffusion coefficient; *DWI,* diffusion-weighted imaging; *MRI,* magnetic resonance imaging; *STIR,* short-T1 inversion recovery.

On MRI, hemangiomas were multilocular and heterogeneous and had high signal intensity on STIR, with signal voids representing phleboliths (Figure 4; see Table III). In addition, hemangiomas infiltrated into the tongue and into the muscles of the floor of the mouth, in addition to extending to the sublingual and submandibular spaces, and the margins of the masses were irregular in some cases (see Table III). On DWI, hemangiomas showed heterogeneous high signal intensity (see Figure 4 and Table III). On MRI, pleomorphic adenomas exhibited heterogeneous high signal intensity on STIR and DWI (see Figure 4 and Table III).

Squamous cell carcinomas and adenoid cystic carcinomas contained solid components and had heterogeneous high signal intensity on STIR (Figure 5; see Table III). In addition, DWI of squamous cell carcinomas and adenoid cystic carcinomas showed heterogeneous high signal intensity (see Figure 5 and Table III). Moreover, the margins of masses were irregular in most cases, unlike those of ranulas (see Table III).

Inflammatory lesions (including abscesses) showed homogeneous high signal intensity on STIR and DWI, but the soft tissues around abscesses had diffuse high signal intensity on STIR and DWI (see Figure 5 and Table III).

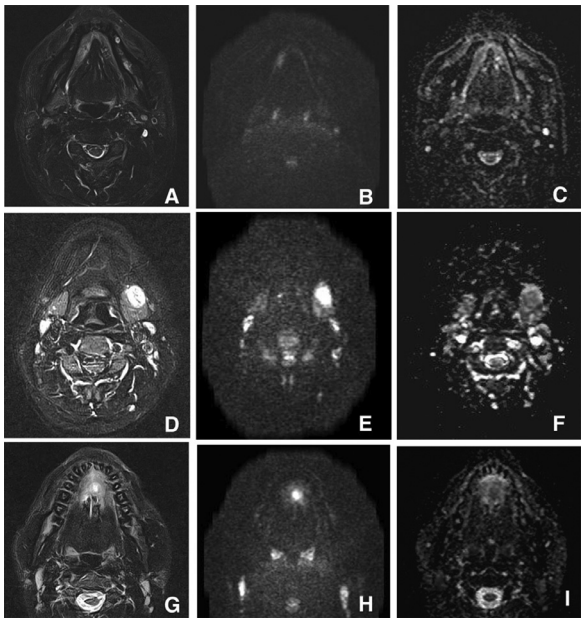

Fig. 5. The MRI findings of a squamous cell carcinoma (A, B, C), an adenoid cystic carcinoma (D, E, F), and inflammation (G, H, I) as examples of lesions with cystic components on STIR (A, D, G), DWI (B, E, H), and the ADC map (C, F, I). The ADC map for the squamous cell carcinoma (C) showed an ADC value of 0.92×10^{-3} mm^2/s. The ADC map of the adenoid cystic carcinoma (F) had an ADC value of 1.10×10^{-3} mm^2/s. The ADC map of the inflammatory lesion (I) had an ADC value of 1.52×10^{-3} mm^2/s. The ADC values for these lesions were significantly lower than those of ranulas in this study. *ADC,* apparent diffusion coefficient; *DWI,* diffusion-weighted imaging; *MRI,* magnetic resonance imaging; *STIR,* short-T1 inversion recovery.

ADC values of DWI for ranulas and other lesions

The ADC values of the ranulas and the other lesions are shown in Table III. The mean ± standard deviation (SD) ADC value of all ranulas was $2.59 \pm 0.31 \times 10^{-3}$ mm^2/s (see Figures 1 and 2 and Table III). The ADC values of ranulas in male and female patients were $2.67 \pm 0.26 \times 10^{-3}$ mm^2/s and $2.50 \pm 0.36 \times 10^{-3}$ mm^2/s, respectively. There was no significant difference between male and female patients in the ADC values of ranulas determined by using the Student *t* test ($P = .690$). In addition, no significant correlation was found between the ADC values of ranulas and age by using Pearson's correlation coefficient ($r = -0.074$; $P = .674$). However, there was a significant difference in the ADC values between simple and plunging ranulas, as determined by using the Student *t* test ($P = .004$) (see Figure 1 and Table III). The ADC values of simple ranulas ($2.52 \pm 0.30 \times 10^{-3}$ mm^2/s) were significantly lower than those of plunging ranulas ($2.79 \pm 0.27 \times 10^{-3}$ mm^2/s).

The mean ± SD ADC values of epidermoid cysts (see Figure 3), thyroglossal duct cysts (see Figure 3),

hemangiomas (see Figure 4), pleomorphic adenomas (see Figure 4), squamous cell carcinomas (see Figure 5), adenoid cystic carcinomas (see Figure 5), and inflammation (see Figure 5) were $1.55 \pm 1.40 \times 10^{-3}$ mm^2/s, $2.16 \pm 0.30 \times 10^{-3}$ mm^2/s, $2.24 \pm 0.66 \times 10^{-3}$ mm^2/s, $1.84 \pm 0.50 \times 10^{-3}$ mm^2/s, $1.02 \pm 0.18 \times 10^{-3}$ mm^2/s, $1.44 \pm 0.20 \times 10^{-3}$ mm^2/s, and $1.53 \pm 0.76 \times 10^{-3}$ mm^2/s, respectively. There were significant differences in the ADC values between ranulas and epidermoid cysts ($P = .010$); malignant tumors, including squamous cell carcinomas and adenoid cystic carcinomas ($P < .001$); and inflammation ($P < .001$), as determined by using the Student t test. However, no significant differences in ADC values were found between ranulas and thyroglossal duct cysts, hemangiomas, or pleomorphic adenomas.

DISCUSSION

The most interesting result of the present study are the characteristic findings of DWI and ADC values in ranulas elucidated for the first time. There was a significant difference in the ADC values between simple and plunging ranulas ($P = .004$). However, there was no significant difference between males and females in the ADC values of ranulas and no significant correlation between the ADC values of ranulas and age. Gender and age would, therefore, not alter the validity of using MRI findings, including DWI and ADC values, clinically for the differential diagnosis of cystic masses or lesions that may have cyst-like components in and around the floor of the mouth.

As expected, there was a significant difference in ADC values between simple and plunging ranulas. The ADC values of simple ranulas were significantly lower than those of plunging ranulas. A possible explanation for this difference is that the fluid in simple ranulas has a higher viscosity because of higher concentrations of protein and other substances. Ranulas with higher ADC values tend to expand into the submandibular spaces if the ranulas are limited to the sublingual spaces.

On DWI, ranulas could be consistently identified as homogeneous, high-signal areas, with relatively less distortion and blurring. The reason for the conspicuity of the lesions on DWI was probably the unrestricted water proton mobility that was of a greater degree than the "T2 shine-through effect." The ADC values in ranulas were relatively high, at $2.59 \pm 0.31 \times 10^{-3}$ mm^2/s. The ADC values of ranulas may reflect the relative free water volume and low protein concentration. Lower protein concentration in ranulas decreases fluid viscosity and increases water proton mobility. The ADC values of ranulas in the present study were higher than those of normal tissues on ADC maps because the mobility of water protons was relatively freer than in other circumstances.

In comparison, all other masses had one or more MRI, DWI, and ADC values different from those of ranulas in the present study. It was possible to objectively differentiate between ranulas and other cystic masses or lesions that may have cyst-like components because there was a significant difference between the ADC values of ranulas and those of the other lesions. As a concrete example, because the ADC values of ranulas were significantly higher, by using ADC values we could differentiate ranulas from epidermoid cysts; malignant tumors, including squamous cell carcinomas and adenoid cystic carcinomas; and inflammation. The MRI findings of ranulas, as reported by Kurabayashi et al.,[6] helped us differentiate ranulas from cystic masses or lesions that may have cyst-like components in the present study. In our investigation, the characteristics of the extent, margin, internal architecture, homogeneity of masses on DWI, and signal intensity on T1WI and STIR in the respective masses were relatively similar to those reported by Kurabayashi et al.[6] However, we considered that it would be very valuable to objectively differentiate ranulas from other cystic masses or lesions that may have cyst-like components by using ADC values.

When only the ADC values were used, we found ranulas to be similar to thyroglossal duct cysts, hemangiomas, and pleomorphic adenomas. Therefore, other MRI findings should also be considered when formulating a differential diagnosis. The characteristic MRI findings of thyroglossal duct cysts included location in the midline of the oral floor and lack of extension into the sublingual glands, unlike the findings in ranulas. In addition, unexpectedly, the internal architecture of some thyroglossal duct cysts was heterogeneous. Hemangiomas were multilocular in many cases and occasionally heterogeneous on STIR and/or DWI, unlike in ranulas. The ADC values of squamous cell carcinomas and adenoid cystic carcinomas in this investigation were similar to those of a previous report.[10] The possible explanation is that the ADC values in cases of massive lesions with solid components are lower than they are in the completely cystic masses. However, to the best of our knowledge, there have been no reports of ADC values of other cystic masses or lesions that may have cyst-like components in and around the oral floor. Data from previous reports of ADC values of nonoral lesions were compared with the present study's data on masses in and around the oral floor. Our data on epidermoid cysts were similar to those from a previous study of the brain, and the ADC values of hemangiomas in the liver were also similar to those of the present study's data.[11-14] In addition, the present study's data on pleomorphic adenomas

were similar to those from a previous report on parotid glands.[15] Therefore, the DWI and ADC values in the present study were acquired appropriately, and this is the first report of ADC values and DWI findings of cystic masses or lesions that may have cyst-like components in and around the floor of the mouth, in addition to those of ranulas, which makes the findings of this study very valuable.

The acquisition of DWI and ADC values is noninvasive, requiring no additional treatment, and the time needed for the acquisition of DWI and the production of ADC maps is about 5 minutes. Therefore, DWI and ADC values should always be acquired for the diagnosis of cystic masses or lesions with cyst-like components of the floor of the mouth.

It has been previously shown that DWI could be of value in the diagnosis of similar conditions in the oral and maxillofacial regions.[9,16] Commonly used in examinations of the brain, the discovery and clinical use of parallel-imaging in DWI can be also effective in examining the oral and maxillofacial regions with their complex anatomy because of the improved spatial resolution and the decrease in susceptibility artifacts.[17,18] The use of DWI and ADC values in the diagnosis of abnormalities in the oral and maxillofacial regions will likely increase.

This study has several possible limitations. First, because the sample size was relatively small, the ADC values might not be standard and accurate. In particular, the various cystic masses or lesions that may have cyst-like components in and around the oral floor other than ranulas were few in number. Therefore, more patients must be evaluated to produce standardized ADC values for certain lesions, such as lymphangioma, lipomas that may be similar to cystic masses on palpation, dermoid cysts, and so on, in the oral and maxillofacial regions. At the same time, surgical procedures were not performed for some benign cysts and benign tumors, such as epidermoid cysts, thyroglossal duct cysts, hemangiomas, and ranulas. However, such lesions can be diagnosed appropriately on the basis of findings from clinical and imaging examinations. In addition, data by gender and age might not necessarily be accurate in the present study sample. In our next study, we plan to evaluate larger sample sizes to confirm the present results and establish the diagnostic criteria for cysts and cyst-like lesions in and around the floor of the oral cavity.

CONCLUSIONS

The characteristic DWI findings and ADC values of ranulas were evaluated, and the data on ranulas and other masses in and around the floor of the mouth, including epidermoid cysts, thyroglossal duct cysts, hemangiomas, pleomorphic adenomas, squamous cell carcinomas, adenoid cystic carcinomas, and inflammatory lesions, were compared. Ranulas were all well-defined, homogeneous masses with high signal intensity on DWI. The mean ± SD ADC of 35 ranulas was $2.59 \pm 0.31 \times 10^{-3}$ mm^2/s. There was a significant difference in ADC values between simple and plunging ranulas. On DWI, most cystic masses or lesions that may have cyst-like components were heterogeneous, and most ADC values were significantly lower than those of ranulas. However, the ADC values of thyroglossal duct cysts and hemangiomas were similar to those of ranulas, although the MRI findings were quite different. The characteristic DWI findings and ADC values of ranulas should be determined accurately, and the data, as those from the present study, will be very useful in the differential diagnosis of many kinds of diseases in and around the floor of the mouth.

REFERENCES

1. Tsuchiya K, Katase S, Yoshino A, Hachiya J. Diffusion-weighted MR imaging of encephalitis. *Am J Roentgenol*. 1999;173:1097-1099.
2. Kono K, Inoue Y, Nakayama K, et al. The role of diffusion-weighted imaging in patients with brain tumors. *Am J Neuroradiol*. 2001;22:1081-1088.
3. Baur A, Stäbler A, Brüning R, et al. Diffusion-weighted MR imaging of bone marrow: differentiation of benign versus pathologic compression fractures. *Radiology*. 1998;207:349-356.
4. Barkovich AJ, Ali FA, Rowley HA, Bass N. Imaging patterns of neonatal hypoglycemia. *Am J Neuroradiol*. 1998;19:523-528.
5. Kito S, Morimoto Y, Tanaka T, et al. Utility of diffusion-weighted images using fast asymmetric spin-echo sequences for detection of abscess formation in the head and neck region. *Oral Surg Oral Med Oral Pathol Oral Radiol Endod*. 2006;101:231-238.
6. Kurabayashi T, Ida M, Yasumoto M, et al. MRI of ranulas. *Neuroradiology*. 2000;42:917-922.
7. Sakamoto J, Imaizumi A, Sasaki Y, et al. Comparison of accuracy of intravoxel incoherent motion and apparent diffusion coefficient techniques for predicting malignancy of head and neck tumors using half-Fourier single-shot turbo spin-echo diffusion-weighted imaging. *Magn Reson Imaging*. 2014;32:860-866.
8. Barchetti F, Pranno N, Giraldi G, et al. The role of 3 Tesla diffusion-weighted imaging in the differential diagnosis of benign versus malignant cervical lymph nodes in patients with head and neck squamous cell carcinoma. *Biomed Res Int*. 2014;2014:532095. https://doi.org/10.1155/2014/532095. Epub 2014 Jun 9.
9. Srinivasan K, Seith Bhalla A, Sharma R, Kumar A, Roychoudhury A, Bhutia O. Diffusion-weighted imaging in the evaluation of odontogenic cysts and tumours. *Br J Radiol*. 2012;85:e864-e870.
10. Kawaguchi M, Kato H, Tomita H, et al. Imaging characteristics of malignant sinonasal tumors. *J Clin Med*. 2017;6. pii: E116.
11. Inan N, Kilinc F, Sarisoy T, Gumustas S, Akansel G, Demirci A. Diffusion weighted MR imaging in the differential diagnosis of haemangiomas and metastases of the liver. *Radiol Oncol*. 2010;44:24-29.
12. Nam SJ, Park KY, Yu JS, Chung JJ, Kim JH, Kim KW. Hepatic cavernous hemangiomas: relationship between speed of intratumoral enhancement during dynamic MRI and apparent diffusion

coefficient on diffusion-weighted imaging. *Korean J Radiol*. 2012;13:728-735.
13. Suzuki C, Maeda M, Matsumine A. Apparent diffusion coefficient of subcutaneous epidermal cysts in the head and neck comparison with intracranial epidermoid cysts. *Acad Radiol*. 2007;14:1020-1028.
14. Severino M, Manara R, Faggin R, Dalle Nogare C, Gamba P, Midrio P. Anorectal malformation and spinal dysraphism: the value of diffusion-weighted imaging in detecting associated intradural (epi)dermoid cyst. *J Pediatr Surg*. 2008;43:1935-1938.
15. Habermann CR, Arndt C, Graessner J, et al. Diffusion-weighted echo-planar MR imaging of primary parotid gland tumors: is a prediction of different histologic subtypes possible. *AJNR Am J Neuroradiol*. 2009;30:591-596.
16. Martínez Barbero JP, Rodríquez Jiménez I, Marthin Noguerol T, Luna Alcalá A. Utility of MRI diffusion techniques in the evaluation of tumors of the head and neck. *Cancers (Basel)*. 2013;5:875-889.
17. Schick F. SPLICE: sub-second diffusion-sensitive MR imaging using a modified fast spin-echo acquisition mode. *Magn Reson Med*. 1997;38:638-644.
18. Alsop DC. Phase insensitive preparation of single-shot RARE: application to diffusion imaging in humans. *Magn Reson Med*. 1997;38:527-533.

Reprint requests:

Yasuhiro Morimoto, Division of Oral and Maxillofacial Radiology, Kyushu Dental University, 2-6-1 Manazuru, Kokurakita-ku, Kitakyushu 803-8580, Japan.
rad-mori@kyu-dent.ac.jp